Fisheries Research
Volume 84, Issue 2, April 2007, Pages 222-232
http://dx.doi.org/10.1016/j.fishres.2006.10.020

Simulation-based study of the combined effect on cod-end size selection of turning meshes by 90° and reducing the number of meshes in the circumference for round fish

Bent Herrmann[a,*], Daniel Priour[b] and Ludvig A. Krag[a]

[a]Danish Institute for Fisheries Research (DIFRES), North Sea Centre, DK-9850 Hirtshals, Denmark
[b]French Institute for Research and Exploitation of the Sea (IFREMER), BP 7029280 Plouzane, France

*: Corresponding author : bhe@dfu.min.dk

Abstract:

FEMNET, a numerical tool based on the finite element method, was used to estimate the shapes of four different designs of trawl cod-ends during fishing operations. Compared to a traditional diamond-mesh cod-end the design differences were the following: (i) the netting orientation was turned by 90° (T90), (ii) the number of meshes in the circumference was reduced by 50% or (i) and (ii) were combined. The cod-end shape estimates were then entered into the simulation tool PRESEMO, to estimate their influence on the selectivity processes in the cod-end. This enabled us to predict how these design alterations – alone or combined – may act on the selectivity of each cod-end under identical fishing conditions. For instance, we predict that for a 110 mm diamond-mesh cod-end the 50% retention length (L50) is increased by nearly 12 cm by both turning the mesh orientation and reducing the number of meshes in the circumference. Of this combined effect we predict that 24% of it is caused by only turning the mesh orientation whereas 71% of the effect stems from only reducing the number of meshes in circumference. The remaining 5% is due to the interaction between the two factors.

Keywords: Cod-end selectivity; T90; PRESEMO; FEMNET

1. Introduction

The ability of a diamond-mesh cod-end to release undersized fish depends on both the mesh size and mesh openings. Underwater observations during trawl fishing have shown that diamond-mesh cod-ends are distorted into a bulbous shape by water pressure acting on the accumulated catch (Stewart and Robertson, 1985). Most of the netting in front of the bulge is stretched and the mesh opening reduced. Only the meshes a few rows just ahead of the catch accumulation are widely open and unobstructed. It is mainly through these meshes that fish escape (Stewart and Robertson, 1985; Wileman et al., 1996). The selective properties of a diamond-mesh cod-end are therefore very dependent on the openness of the mesh rows close to the accumulated catch and on catch size. Experimental work by Reeves et al. (1992) and by Galbraith et al. (1994) showed that reducing the number of meshes around the cod-end circumference could increase L50 for round fish in the North Sea trawl fishery. This has been recognized in the legislation (EU Regulation no. 850/98) which prescribes an upper limit of 100 meshes in the circumferences. Experimental work (Dahm et al. 2004) has indicated that turning the diamond-mesh netting by 90 degrees (T90) may increase L50, compared to a similar cod-end with normal netting orientation. Considering normal netting orientation (T0), it seems that mesh resistance to opening tends to close the meshes. By turning the netting by 90 degrees this mechanism reverses into a mesh resistance to closing, which facilitates juvenile roundfish escapement through the meshes. The netting knot size, defined by the knot type and twine characteristics, may also contribute to the benefit of turning the netting by 90 degrees. The mesh openness at a given position along the cod-end axis is defined by the diameter of the cod-end at that position and the number of meshes around. As a rule the shape of a diamond-mesh cod-end depends on the force distribution over the netting, including the drag on the catch and the resistance of the netting to either closing or opening the mesh (Priour, 2001). Thus, the mesh openness will be different for two identical cod-ends, where one has its netting turned by 90 degrees. Fig. 1 also demonstrates this difference between normal netting and T90 netting stressed by the same forces along the vertical axis.

In the Baltic Sea cod (*Gadus morhua*) fishery, T90 cod-ends have since 2006 been imposed by legislation (EU Regulation no. 2187/2005) in combination with a reduction of the number of meshes in the circumference from 100 to 50, and a minimum 110 mm mesh size. Thus the implementation of T90 in the Baltic Sea cod fishery is not a single-factor effect but a combined effect: i) turning the meshes by 90 degrees; ii) reducing the number of meshes in the circumference by 50%. Now, these two factors may interact either positively or negatively. This raises questions:

(i) To what extent do each of these factors contribute to the total effect on the size selectivity of the diamond-mesh cod-end?

(ii) Is the interaction between the two factors positive or negative and how influential is it?

The objective of this paper is to address these questions. Because both the factors influence selectivity by affecting the degree of openness of the diamond-shaped meshes, a sub-objective is to establish a quantitative model between cod-end mesh size, mesh openness and sizes of fish liable to escape through the mesh. To fulfil the objectives we used the cod-end simulation program, PRESEMO (Herrmann; 2005a) to estimate the selectivity of different cod-end designs. To estimate the cod-end shapes for different catch weights, as required to run PRESEMO, we used FEMNET (Priour; 1999; 2001; 2005), a numerical tool based on the finite element method to calculate shapes of netting structures like trawl cod-ends. Instead of running a case study for the Baltic Sea cod fishery we performed the case study on haddock (*Melanogrammus aeglefinus*) in the North Sea trawl fishery because of the higher quality data available and our greater experience in using PRESEMO for this fishery (Herrmann (2005b); Herrmann and O'Neill (2005); Herrmann and O'Neill (2006); Herrmann et al. (2006)). This way we believe our predictions are more reliable. However, we assume that the relative effects for both haddock and cod are quite similar.

2. Materials and methods

2.1. Experimental design and statistical model

We implemented models of four different cod-ends to predict and elucidate what effect turning the netting by 90 degrees and reducing the number of meshes in the circumference by 50% would have on cod-end selectivity. We assume that all four gears are made of the same 110 mm diamond-mesh netting (120.2 in full mesh) and 4 mm PE double twine. All cod-ends are 50 meshes long. The four designs T0X100, T0X50, T90X100 and T90X50 are described in Table 1: T0X100 being the reference cod-end with normal netting orientation and 100 meshes in the circumference; T0X50 consisting of normal netting orientation and 50 meshes in the circumference; T90X100 consisting of netting turned by 90 degrees and 100 meshes in the circumference; and T90X50 of netting turned by 90 degrees and 50 meshes in the circumference. For each cod-end we simulate 1000 hauls leading to 4000 single-haul estimates of L50 and selection range SR (L75 – L25). From these data we are able to predict the mean effects on cod-end selectivity of: i) reducing the number of meshes in the circumference; ii) turning the mesh by 90 degrees; iii) the combined effect of both. Fryer (1991) developed a statistical model to estimate the mean selection from individual hauls taking between-haul variation into account and enabling deduction of fixed effects. We used the software tool EC-WEB (http://www.constat.dk/ecwebsd) which implements the model of Fryer (1991) to analyse the simulated haul data. For this purpose we needed to formulate a statistical model which complies with the input format of EC-WEB, according to the following model:

$$\begin{aligned} L50 &= F_{0.1} + F_{1.1} \times I_1 + F_{2.1} \times I_2 + F_{3.1} \times I_3 \\ SR &= F_{0.2} + F_{1.2} \times I_1 + F_{2.2} \times I_2 + F_{3.2} \times I_3 \end{aligned} \qquad (1)$$

I_1, I_2 and I_3 are presence factors (0 or 1) for three fixed effects, and stand for a reduction by 50% of the number of meshes in the cod-end circumference, for turning the netting by 90 degrees and for the combination of the two previous ones, respectively. The values of I_1, I_2 and I_3 for the different gears (T0X100, T0X50, T90X100 and T90X50) are listed in Table 2. $F_{0.1}$ and $F_{0.2}$ thus quantify the mean L50 and mean SR for the basic design T0X100. $F_{1.1}$ and $F_{1.2}$ quantify the mean effect of I_1. $F_{2.1}$ and $F_{2.2}$ quantify the mean effect of I_2. $F_{3.1}$ and $F_{3.2}$ quantify the mean effect of I_3. The interaction effect of simultaneously reducing the number of meshes of the circumference and turning the netting by 90 degrees can be quantified by $F_{3.1} - (F_{2.1} + F_{1.1})$ for mean L50 and by $F_{3.2} - (F_{2.2} + F_{1.2})$ for mean SR. The percentage effect of reducing the number of meshes around from the total effect of both reducing the number of meshes of the circumference and turning the netting by 90 degrees is quantified by $100x(F_{1.1}/F_{3.1})$ for mean L50 and by $100x(F_{1.2}/F_{3.2})$ for mean SR. The percentage effect of turning the netting by 90 degrees from the total effect of both reducing the number of meshes of the circumference and turning the netting by 90 degrees is quantified by $100x(F_{2.1}/F_{3.1})$ for mean L50 and by $100x(F_{2.2}/F_{3.2})$ for mean SR. The percentage interaction effect, when both reducing the number of meshes of the circumference and turning the netting by 90 degrees, of the total effect is quantified by $100x((F_{3.1} - (F_{2.1} + F_{1.1}))/F_{3.1})$ for mean L50 and by $100x((F_{3.2} - (F_{2.2} + F_{1.2}))/F_{3.2})$ for mean SR.

2.2. Calculation of cod-end shapes

The shapes are calculated with a 3D Finite Element Method model (FEMNET) designed for flexible structures and based on triangular elements for the netting (Priour 1999, 2005). FEMNET takes into account the twines' tension, the drag force on the net when towed, the pressure created by

the fish in the cod-end (Priour and Herrmann 2005), the twine contact when the meshes are closed, the mesh opening stiffness and the bending stiffness of the net.
The model must take into account the difference of nettings mechanical behaviour when in normal orientation and when turned by 90 degrees. We model the mesh resistance to opening by a momentum *C* acting between the mesh bars trying to keep the netting closed (Θ = 0.0, Fig. 2). Increasing Θ will thus be counteracted by increasing *C* from 0.0. We assume that *C* is proportional to the angle between the mesh bars (Priour 2001):

$$C = G \times \theta \tag{2}$$

The mesh opening stiffness G as introduced by (2) has not been measured on fishing nets as far as we know. Sala et al. (2004) developed a specific methodology based on the beam theory (Timoshenko, S.P. and Goodier, J.N., 1982) for the measurement of the mesh opening stiffness. They quantified this characteristic through the mesh bar bending stiffness (*EI*). We have derived (see Appendix 1) a relation between the mesh opening stiffness *G* (in Nm/rad) used in FEMNET and the mesh bar bending stiffness *EI* (in Nm^2) as measured by Sala et al. (2004):

$$G = \frac{12 \times EI}{m} \tag{3}$$

where *m* (in m) is the full mesh size which is equal to the inside mesh size (*mi*) plus one knot length (*kl)* (Fig. 2).
The cod-end shape data required for PRESEMO simulations, were calculated for 13 catch weights for each of the gears listed in Table 1: 60, 78, 100, 130, 167, 216, 280, 361, 467, 603, 779, 1300 and 2000 kg. Because the calculations of cod-end shapes for small catch weights are uncertain, the shapes for catches below 60 kg were assumed to be the same as for 60 kg. The towing speed was assumed to be 3.4 knots in all shape calculations.

2.3. Simulation of selection and comparison with empirical results
PRESEMO requires information on fish behaviour, escape processes, fish population structure and fish morphology. Herrmann and O'Neill (2005) outlined a protocol for using PRESEMO where between-haul variation is taken into account. They used the protocol to study the selectivity of haddock for catch weights up to 500 kg. Herrmann et al. (2006) used a modified version of this protocol to study the effect of cod-end round straps on the selectivity of haddock for a larger range of catch weights. In this study we use the latter protocol for all simulations, thus the same PRESEMO settings for fish behavior, escape processes, fish population structure and fish morphology as used by Herrmann et al. (2006) (see this reference for detailed information). For designs T0X100 and T0X50 we compared results with those predicted by the two empirical models described in Galbraith et al. (1994). For design T0X100 we also compared the results achieved with single-haul results reported in Kynoch et al. (2003). These results are biased by the use of a thicker twine (5 mm) which leads to a change of +2.1 cm in L50 and +0.3 cm in SR based on model 4 reported in Herrmann and O'Neill (2006).

2.4. Model describing the maximum length (Lmax) to allow a fish to escape through a mesh
This section formulates a model which predicts the maximum length to allow a roundfish to escape through a diamond-shaped mesh without deforming either the mesh or itself. Let us assume that the largest fish cross-section can be described by an ellipse with the same height (*h*) and width (*w*) as the fish. Fig. 3 shows the shape of a diamond-mesh inside size (*mi)* and the size of the largest

elliptical cross-section with the given h-w-ratio that can pass through the mesh. The shape of the diamond-mesh is described by its openness ratio (*op*), which is the ratio between lateral mesh opening (2 x *b*) in Fig. 3 and inside mesh size (*mi*) in Fig. 3. Thus *op* can be expressed by:

$$op = \frac{2 \times b}{mi} = \sin(\Theta) \tag{4}$$

where *op* is a number between 0.0 and 1.0. Assuming that the width (*w*) and the height (*h*) are both proportional to the length (*l*) of the fish we write:

$$\begin{aligned} w &= wf \times l \\ h &= hf \times l \end{aligned} \tag{5}$$

wf and *hf* are constants of proportionality. Based on the above assumptions, Appendix 2 shows, that *Lmax* can be expressed by:

$$l1(mi, op, wf, hf) = mi \times op \times \sqrt{\left(\frac{(1 - op^2)}{hf^2 \times (1 - op^2) + wf^2 \times op^2} \right)}$$

$$l2(mi, op, wf, hf) = mi \times op \times \sqrt{\left(\frac{(1 - op^2)}{wf^2 \times (1 - op^2) + hf^2 \times op^2} \right)} \tag{6}$$

$$L\max(mi, op, wf, hf) = \begin{cases} l1 & \forall \quad l1 \geq l2 \\ l2 & \forall \quad l2 > l1 \end{cases}$$

Fig. 4 plots *Lmax* versus *op* for a 110 mm mesh size using the mean morphological data for haddock used in Herrmann et al. (2006). From Fig. 4 it is clear that whether a roundfish passes through a diamond-mesh without deforming it is highly dependent on mesh openness. The *Lmax* variation along the cod-end, in relation to the weight of the catch can be used to give a first indication on whether a cod-end design can be expected to facilitate roundfish escapement or not.

3. Results

3.1. Shape calculations and values for Lmax

Fig. 5 shows plots, obtained with PRESEMO, of the shapes for cod-end design: T0X100, T0X50, T90X100, T90X50 for three different catch weights: 100, 500, 1000 kg. For 500 and 1000 kg the shapes are interpolations of those calculated by FEMNET. It is clear from these plots that the shapes are quite different. On each plot there are four marks: Mark 1 represents the position of the catch edge; mark 2 represents a position 0.5 m in front of the catch; mark 3 represents a position 1.0 m in front of the catch, and mark 4 represents a position 1.5 m in front of the catch. Let's compare plots for T0X100 with T90X100 and T0X50 with T90X50 : as expected, it is clear that the shapes of the two cod-ends — one having normal netting direction and the other one's netting being turned by 90 degrees — will be different owing to the difference in mesh resistance, which tends to either close or open the mesh as suggested in the introduction. Using the formulas (4) for the maximum mean escapement length (*Lmax*) we can make a rough first quantification of the influence on roundfish escapement caused by the difference in cod-end shapes. Table 3 lists *Lmax* for different catch weights up to 1000 kg at: mark 1 (*Lmax1*), mark 2 (*Lmax2*), mark 3 (*Lmax3*), mark 4 (*Lmax4*) for each of the four cod-end designs. It is clear that for all cod-end designs and catch weights investigated *Lmax* is always higher at the catch edge (mark 1), reducing as the distance from the catch edge increases (towards mark 4). The value of *Lmax1* is likely to be the most pertinent of the four, since the underwater observations referred to by Stewart and Robertson (1985) and by Wileman et al. (1996) indicate that most escapement of roundfish occurs through the few mesh rows just in front of the catch. Fig. 6 plots *Lmax* versus catch weight at mark 1 – 4 for the four different cod-end designs. *Lmax* is obviously smaller for the T0X100 design. The influence on *Lmax* at catch edge by turning the meshes (T0X100 versus T90X100 or T0X50 versus T90X50) compared to reducing the number of meshes in the circumference (T0X100 versus T0X50 or T90X100 versus T90X50), indicates that the highest influence is exerted by the latter and being most profound for small catch weights. For higher catch weights the plot indicates that *Lmax* at the catch edge seems to converge almost towards the same value for all the designs. For positions further away from catch edge, especially at marks 3 and 4, the tendency for *Lmax* is not so clear. Overall, however *Lmax* is always larger for the turned mesh design compared to the similar standard design (T90X100 to T0X100 and T90X50 to T0X50). This tendency is also confirmed by a detailed inspection of the data provided in Table 3.

3.2. Selectivity simulation results for each cod-end design and comparison with empirical results.

Fig. 7 plots L50 (left) and SR (right) versus the total catch weight for each of the 1000 simulated hauls for each cod-end design T0X100, T0X50, T90X100, T90X50 (from top). The grey curves are the plots of the second-order polynomial regression of L50 versus total catch weight. Mean selection parameters based on the 1000 hauls simulated for each design are summarized in Table 4 where designs T0X100 and T0X50 are also compared to predictions using empirical models from Galbraith et al. (1994). For design T0X100 we also compare the results with the mean estimates reported in Kynoch et al. (2003). From Table 4 it is seen that our simulations predict a mean L50 of 31.6 cm for design T0X100 and 40.2 cm for design T0X50, whereas Galbraith's models predict 30.9 cm and 30.2 cm for design T0X100 and 39.2 cm and 40.2 cm for design T0X50. The compensated single-haul results from Kynoch et al. (2003) are also included in Fig. 7 (upper plots) marked □. The simulated L50 values are in reasonable agreement with the empirical results (Table 4 and Fig. 7). For SR our simulations predict mean values of 5.9 cm for design T0X100 and 6.6 cm for design T0X50 compared to 5.6 cm and 6.9 cm, respectively, using the models of Galbraith et al. (1994). We thus achieve a reasonable agreement with the empirical results even through our overestimate SR results compared to the compensated results by Kynoch et al. (2003).

By comparing the mean results of the simulations for the different designs we predict an increase in L50 by about 12 cm when both the mesh orientation is turned by 90 degrees and the number of meshes in the circumference is reduced (design T0X100 versus design T90X50). For the designs with a standard number of meshes in the circumference (design T0X100 and T90X100) Fig. 7 indicates a tendency for L50 to increase with catch weight. L50 predicted by the regressions for the different cod-end designs clearly emphasizes this phenomenon (Table 5). L50 decreases slightly for design T0X50 (Table 5), while it remains almost constant for design T90X50. The cause of these tendencies for design T0X50 and T90X50 is probably that the mesh deformation by the fish is taken into account in the simulations for small catches made at the beginning of the haul (see Herrmann and O'Neill; 2005). For these designs this effect more than compensates for the smaller mesh opening at the beginning of the process which is inversely reflected in *Lmax* (section 3.2). An explanation for the substantial difference between the catch weight dependency found between T0X100 and T0X50 shapes could indeed be related to the difference in dependency of mesh openness on catch weight. Considering a diamond-mesh cod-end, the diameter just ahead of the catch increases with the catch, up to a certain limit. Once this limit achieved, the diameter remains constant whatever the catch increase (Herrmann et al., 2006). When there are as many as 100 open meshes along the cod-end circumference it takes a far greater volume of catch to reach the maximum diameter compared to a cod-end having only 50 open meshes along the circumference. This means that mesh openness will be affected over a larger range of catch weight for the T0X100 cod-end compared to the T0X50 cod-end. Another important mechanism also related to the observed phenomena is that for the same cod-end diameter the cod-end with fewer meshes will have a bigger circumferential opening of meshes (2b in Fig. 2) than the cod-end with more meshes. Both these aspects are clearly demonstrated in Fig. 6 (top-left plot) where the dependency on catch weight of *Lmax* just ahead of the catch is plotted for the cod-ends (■: for T0X100; □: for T0X50). For T0X50 *Lmax* is already very close to the maximum value for a 60 kg catch while for T0X100 *Lmax* has not yet reached the maximum value. As *L50* is in some way a result of the integration of *Lmax* with respect to catch weight we believe that the mechanisms outlined above can quite explain the difference in dependency on catch weight found between the T0X100 and T0X50 cod-ends.

3.3. Results for the statistical model.

We estimate the values for the model parameters using the statistical model (1) with the selection parameter estimates from each of the 4000 simulated hauls in the statistical tool EC-web (Table 6). All parameters are found to be highly significant (p-value < 0.05) (Table 6). Based on these parameters and the expressions formulated in section 2.1 we are able to quantify the effect of the two factors: i) reduction in number of meshes in the circumference; ii) turning netting orientation; and of their interaction. Table 7 lists the results for L50 increase and shows that 24% of its increase is caused by turning the mesh whereas 71% of the increase rest on reducing the number of meshes in the circumferences. The remaining 5% is due to the interaction effect between the two factors. We predict that turning the meshes by 90 degrees tends to decrease SR, while reducing the number of meshes in the circumference tends to increase SR. But the effects are small on mean SR (all less than 1 cm).

4. Discussion

The use of simulation tools FEMNET and PRESEMO enabled us to conduct a simulation based study of the expected effect on haddock selection when using netting turned by 90 degrees and/or reducing by 50% the number of meshes in the cod-end circumference. This study concerns haddock, but we expect similar results for other roundfish species like cod because they have similar shapes and are fished in the same way.

The simulation methods described here have obvious advantages relative to experimental fishing. It is possible to run a very large number of hauls under varying fishing conditions, where each configuration is exposed to identical varying conditions, thus making explicit results comparable. The maximum total catch weight considered for this study was 1000 kg. For larger catch weights it is possible that the effects predicted on selectivity may be slightly different. Another advantage of implementing the simulation methods, compared to experimental fishing, is that it gives the possibility to conduct rapid and cost-effective tests on a new cod-end design. However we have to be cautious when using this approach for a given fishery because it then will be necessary to make sure that the PRESEMO input parameters pertain to the fishery in question. Now, the predictions in this study, at least for the T0X100 and T0X50, seem to be reasonable as indicated by the comparisons made with empirical results (table 4; Fig. 7 (top-left)).

In FEMNET the specific mechanical properties of the netting have been introduced to represent the differences between the standard orientation and the T90. This has been done on several assumptions: i) Firstly, that the netting is modelled as diamond-mesh. Alternatively the netting could be modelled as a hexagonal mesh taking the knot length (*kl*) into account. On Fig.1-2 it can be seen that the knot length could be two sides of the hexagon, the mesh bars forming the four other sides. However for a 110 mm inside mesh size in double 4 mm knotted netting the knot length is so small compared to mesh bar length (m/2) that we assume the diamond-mesh approximation is valid to the present study; ii) Secondly, in the modelling of the netting the mesh bars are assumed to be straight bars (Appendix 1). An alternative could be to consider them as beams, as described by O'Neill (1997). Due to the tension in the mesh bars resulting from the drag on the catch we assume that the straight-bar approximation is acceptable here; iii) Lastly, the mesh opening resistance is introduced by a momentum between the mesh bars (Fig. 2). We found a relation between our modelling and the work of Sala et al. (2004) and O'Neill (1997) and therefore find this assumption acceptable.

The way we have modelled mesh resistance to closing for the turned mesh cod-ends implies that there is no loss of resistance (relaxation) after the mesh has been under tension over longer periods as during fishing operations. The positive effect of turning mesh orientation will be less than predicted, in this study, if relaxation occurs. On the contrary, relaxation will have no influence on the effect of reducing the number of meshes in the circumference. These aspects could all affect the reliability of our estimation of the shape of cod-ends made of meshes turned by 90 degrees. Therefore, experimental verification, for instance flume tank tests, conducted on at least one cod-end design would be beneficial.

Design T90X50 is the legal alternative to the Bacoma cod-end (EU Regulation no. 850/98) in the Baltic Sea Cod fishery. This study has shown that the 50% reduction in number of meshes in the cod-end circumference contributes three times more to the overall increase of L50, relative to the standard 110mm cod-end (design T0X100), than turning the meshes by 90 degrees. The improved selectivity of the cod-end currently used in the Baltic could be mainly associated with the reduced number of meshes in the circumference. This observation should be recognized especially if the turned mesh cod-end is to be introduced as a selective alternative in other waters.

Acknowledgement
This study was carried out with the financial support from the Commission of the European Communities, specific RTD programme Quality of Life and Management of Living Resources, “PREMECS II: Development of predictive model of cod-end selectivity”. It does not necessarily reflect the Commission’s view and in no way anticipates its future policy in this area. Financial support was also given from project SELTRA financed by the Directorate for Food, Fisheries and Agri Business of Denmark. The authors are anxious to thank Mariana B. Horsten and Bo Lundgren both from DIFRES and Patricia Barthelemy from IFREMER for invaluable grammatical assistance in drafting the present text.

Appendix 1

Formula (3) is derived for the relation between the mesh opening stiffness *G* used in FEMNET and the mesh bar bending stiffness *EI* as measured by Sala et al. (2004). We start by assuming that the equilibrium of a mesh bar emerging from the knot follows the thin beam theory (Timoshenko, S.P. and Goodier, J.N., 1982). When the deformation is small and there is no tension in the beam, the equilibrium of the momentum *C* and force couple *Q* at the knots gives (Fig. 8):

$$C = \frac{Q \times m}{4} \tag{7}$$

From the thin beam theory we have:

$$y = -\frac{Q \times m^3}{96EI} \tag{8}$$

The angle Θ is related to the deformation by:

$$\mathbf{sin}(\Theta) = \frac{2\mathrm{y}}{\mathrm{m}} \text{ Which leads to } \sin(\Theta) = \frac{Q \times m^2}{48EI} \qquad \text{And to } C = \sin(\Theta)\frac{12EI}{m} \tag{9}$$

This means that the mesh opening stiffness *G* by using (2) can be expressed by:

$$G = \frac{C}{\Theta} = \frac{\sin(\Theta)}{\Theta} \times \frac{12EI}{m} \tag{10}$$

As the ratio of $\sin(\Theta)/\Theta$ is between 0.896 and 1.0 for Θ less than 45°, this means that this ratio is quite close to 1.0 and therefore (10) reduces to (3).

Appendix 2

Formula (6) is derived for *Lmax* for a fish of elliptical cross-section to pass through the mesh. We start with a diamond-shaped mesh and assume that the fish cannot distort the shape of the mesh nor itself when trying to pass through the mesh. Referring to Fig. 3 the equation for the fish cross section may be written as:

$$\frac{4x^2}{w^2}+\frac{4y^2}{h^2}=1 \tag{11}$$

Referring to Fig. 3 and formulas (4) the equation for the mesh bar in first quarter (x and y both positive) can be written as:

$$y=\frac{op\times mi}{2}\times\left(1-\frac{2x}{mi\times\sqrt{1-op^2}}\right) \tag{12}$$

Inserting (12) in (11) we can derive the condition for intersection between the ellipse (fish cross section) and the mesh bar. This leads to:

$$\frac{4x^2}{w^2}+\frac{4op^2\times mi^2}{4h^2}\times\left(1-\frac{2x}{mi\times\sqrt{1-op^2}}\right)^2=1$$

$$\Updownarrow \tag{13}$$

$$x^2\times\left(\frac{4}{w^2}+\frac{4op^2}{h^2\times\left(1-op^2\right)}\right)+x\times\left(-\frac{4mi\times op^2}{h^2\times\sqrt{1-op^2}}\right)+\left(\frac{op^2\times mi^2}{h^2}-1\right)=0$$

(13) is a polynomial of second order. The biggest fish that can escape can only do so by coming into contact with the mesh bars (the mesh bar is tangent to the ellipse). This condition can be expressed by a unique real solution for (13). The condition for this is that the determinant D to (13) is zero:

$$\begin{cases} D=B^2-4A\times C \\ A=\dfrac{4}{w^2}+\dfrac{4op^2}{h^2\times\left(1-op^2\right)} \\ B=-\dfrac{4mi\times op^2}{h^2\times\sqrt{1-op^2}} \\ C=\dfrac{op^2\times mi^2}{h^2}-1 \end{cases}$$

$$\Downarrow \tag{14}$$

$$D=\frac{16mi^2\times op^4}{h^4\times\left(1-op^2\right)}-16\times\left(\frac{1}{w^2}+\frac{op^2}{h^2\times\left(1-op^2\right)}\right)\times\left(\frac{op^2\times mi^2}{h^2}-1\right)$$

(14) and the condition $D = 0$ leads to:

$$\frac{mi^2 \times op^4}{h^4 \times \left(1-op^2\right)} - \frac{op^2 \times mi^2}{w^2 \times h^2} - \frac{op^4 \times mi^2}{h^4 \times \left(1-op^2\right)} + \frac{1}{w^2} + \frac{op^2}{h^2 \times \left(1-op^2\right)} = 0$$
$$\Downarrow \qquad (15)$$
$$\left(1-op^2\right) \times \left(h^2 - op^2 \times mi^2\right) + op^2 \times w^2 = 0$$

Using the same procedure where the fish is turned 90 degrees around its axis (which means interchange *h* and *w* for the ellipse given by (11)) leads to:

$$\left(1-op^2\right) \times \left(w^2 - op^2 \times mi^2\right) + op^2 \times h^2 = 0 \qquad (16)$$

Inserting (5) in (15) and (16) leads to:

$$\begin{cases} \left(1-op^2\right) \times \left({h_f}^2 \times l^2 - op^2 \times mi^2\right) + op^2 \times {w_f}^2 \times l^2 = 0 \\ \left(1-op^2\right) \times \left({w_f}^2 \times l^2 - op^2 \times mi^2\right) + op^2 \times {h_f}^2 \times l^2 = 0 \end{cases}$$
$$\Downarrow$$
$$l1 = op \times mi \times \sqrt{\frac{1-op^2}{\left(1-op^2\right) \times {h_f}^2 + op^2 \times {w_f}^2}} \qquad (17)$$
$$l2 = op \times mi \times \sqrt{\frac{1-op^2}{\left(1-op^2\right) \times {w_f}^2 + op^2 \times {h_f}^2}}$$

Where *l*1 is for the fish op-right and *l*2 is for the fish turned 90°. The maximum escapement length *Lmax* then is the maximum of *l*1 and *l*2 thus:

$$L\max = \begin{cases} l1 & \forall \quad l1 \geq l2 \\ l2 & \forall \quad l2 > l1 \end{cases} \qquad (18)$$

(17) and (18) together is identical to (6) thus we have derived this.

References

Dahm, E., 2004 (convener). Evaluate the recent (last 5 years) codend mesh selection experiments dealing with bottom trawls used in the Baltic Sea for cod which used either turned meshes and/or BACOMA windows. With emphasis on estimating selectivity parameters, experimental design and modelling/statistical analysis. Report of the ICES Fisheries Technology Committee Working Group on Fishing Technology and Fish Behaviour, Gdynia (Poland), ICES CM 2004/B.05 Ref. ACE: pp 24 pp.

Herrmann, B., 2005a. Effect of catch size and shape on the selectivity of diamond mesh cod-ends I. Model development. Fish. Res. 71, 1-13.

Herrmann, B., 2005b. Effect of catch size and shape on the selectivity of diamond mesh cod-ends II. Theoretical study of haddock selection. Fish. Res. 71, 15-26.

Herrmann, B. and O'Neill, F.G., 2005. Theoretical study of the between-haul variation of haddock selectivity in a diamond mesh cod-end. Fish. Res. 74, 243-252.

Herrmann, B. and O'Neill, F.G., 2006. Theoretical study of the influence of twine thickness on haddock selectivity in diamond mesh cod-ends. Fish. Res. 80, 221-229.

Herrmann, B., Priour, D., Krag, L.A., 2006. Theoretical study of the effect of round straps on the selectivity in a diamond mesh cod-end. Fish. Res. 80, 148-157.

Galbraith R.D., Fryer R.J., Maitland K.M.S., 1994. Demersal pair trawl cod-end selectivity models. Fish. Res. 20, 13-27.

O'Neill F.G., 1997, Differential equations governing the geometry of a diamond mesh codend of a trawl net, J. Appl. Mech., March 1997, Vol. 64 / 7, 453, p. 1631-1648.

Priour, D., 1999. Calculation of net shapes by the finite element method with triangular elements. Commun. Numer. Meth. 15, 755-763.

Priour, D., 2001. Introduction of mesh resistance to opening in a triangular element for calculation of nets by the finite element method. Commun. Numer. Meth. 17, 229-237.

Priour, D., 2005. FEM modelling of flexible structures made of cables, bars and nets. Proceedings of the 12th international congress of the international maritime association of the mediterrranean IMAM 2005, Lisbon, 26-30 September 2005, V.2, pp 1285-1292, ISBN 0 415 39036 2.

Priour, D., Herrmann, B., 2005, Catch shape in codend, DEMAT05, Busan, 23-25 November 2005. Proceedings of the 7th international workshop on methods for the development and evaluation of maritime technologies, Busan, 23-26 November 2005, pp 41-58, ISBN 89-89382-22-X 93520 ISSN 0945-0874.

Reeves, S.A., Armstrong, D.W., Fryer, R.J., Coull, K.A., 1992. The effects of mesh size, cod-end extension length and cod-end diameter on the selectivity of Scottish trawls and seines. ICES J. Mar. Sci. 49, 279-288.

Sala A., O'Neill F.G., Buglioni G., Cosimi G., Palumbo V., Lucchetti A., 2004. Development of an experimental method for quantifying the resistance to opening of netting panels. Report of the ICES Fisheries Technology Committee Working Group on Fishing Technology and Fish Behaviour, Gdynia (Poland), ICES CM 2004/B.05 Ref. ACE: 189 pp.

Stewart, P. A. M. and Robertson, J. H. B., 1985. Scottish Fisheries Research Report No. 33, 15 pp.

Timoshenko, S.P. and Goodier, J.N., 1982. Theory of elasticity. McGraw-Hill, ISBN: 07-085805-5

Wileman, D., Ferro, R. S. T., Fonteyne, R., Millar, R. B. (editors), 1996. Manual of methods of measuring the selectivity of towed fishing gears. ICES Coop. Res. Rep. No. 215.

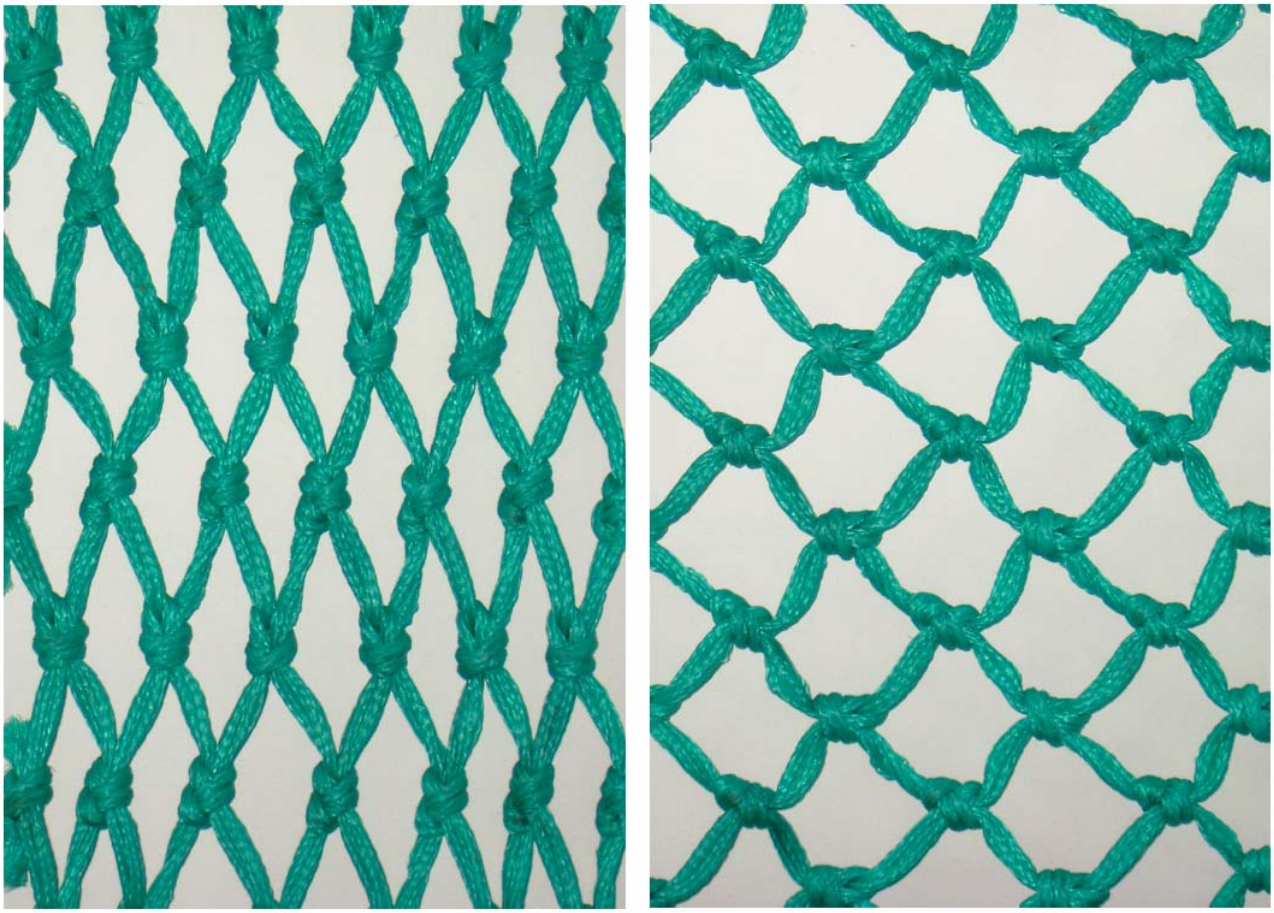

Fig. 1: Difference in mesh opening for the same netting stressed vertically by the same load. Left used as normal netting and right used as T90 netting. Mesh size is 110 mm and twine thickness 5 mm double.

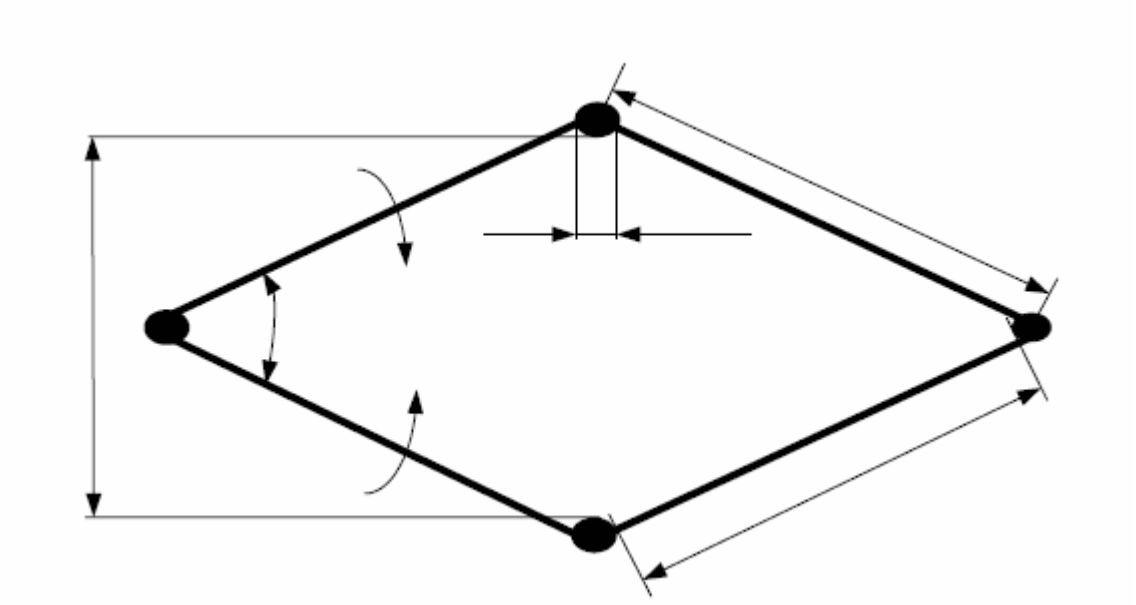

Fig. 2: Diamond-mesh as modelled in FEMNET by straight bars. When trying to open the mesh by increasing the mesh opening angle *2Θ* from zero the mesh counteracts with moments *C* while trying to keep *2Θ* to zero. *mi* is the inside mesh size. *kl* is the knot length. *m* is the full mesh size *(mi + kl)*.

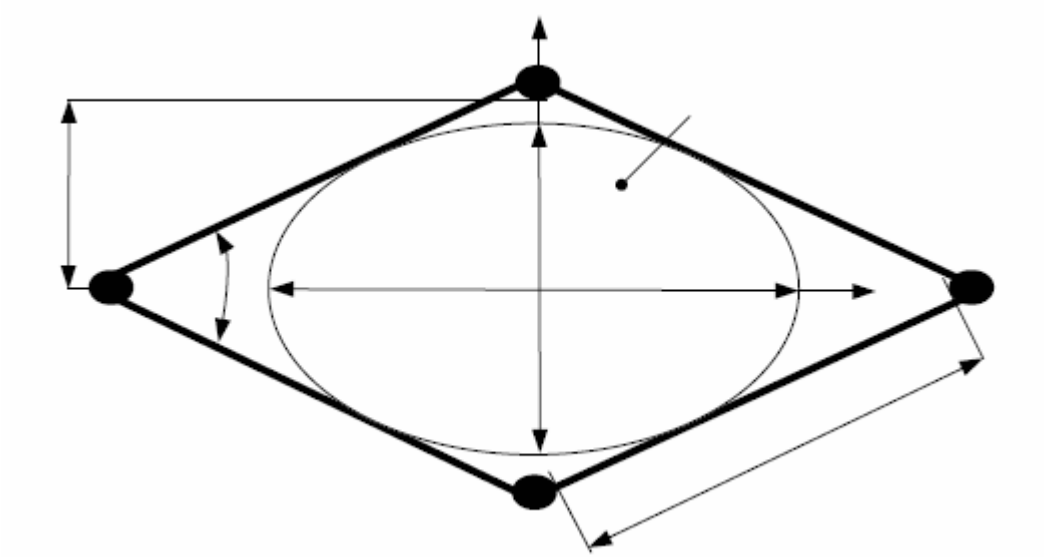

Fig. 3: Diamond-mesh and fish with elliptical cross-section. Mesh size *mi*. Lateral mesh opening *2xb*. Fish height *h* and fish width *w*.

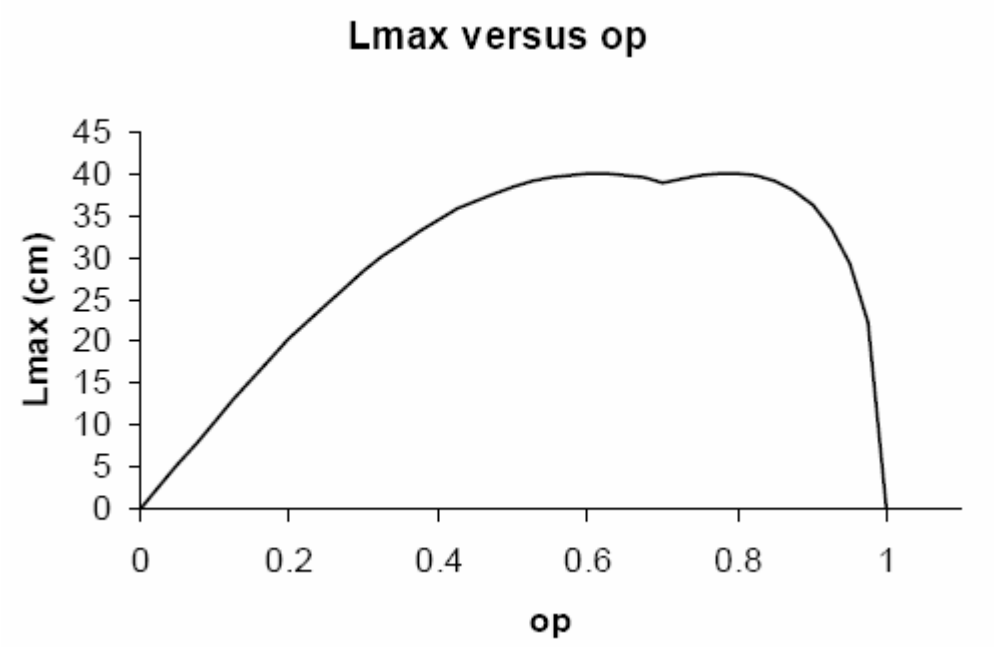

Fig. 4: *Lmax* versus mesh opening ratio *op*.

Design	100 kg catch weight	500 kg catch weight	1000 kg catch weight
T0X100	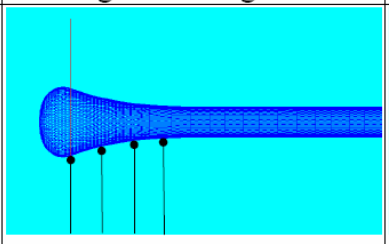	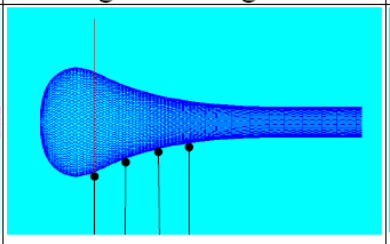	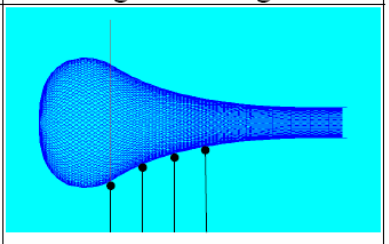
T0X50	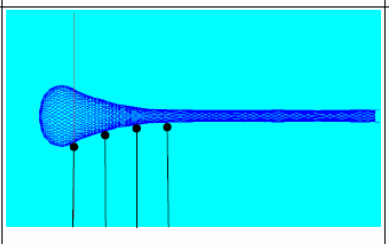	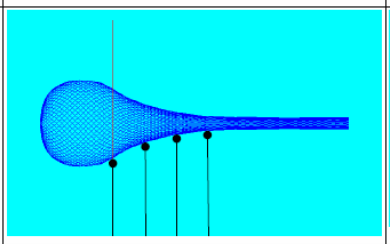	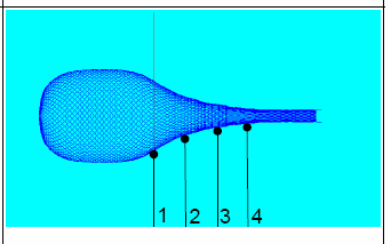
T90X100	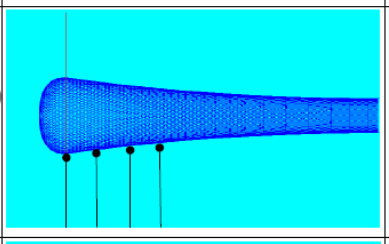	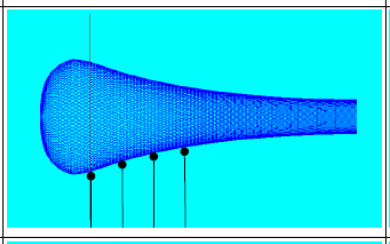	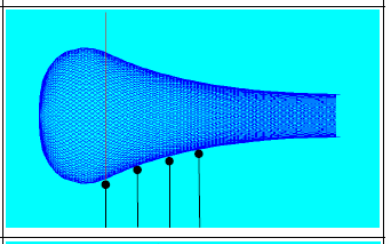
T90X50	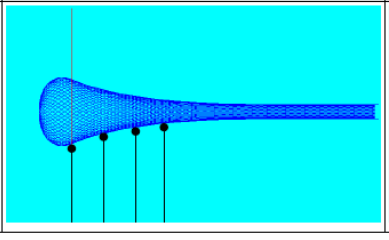	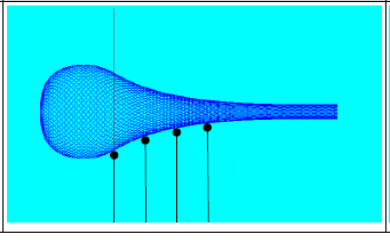	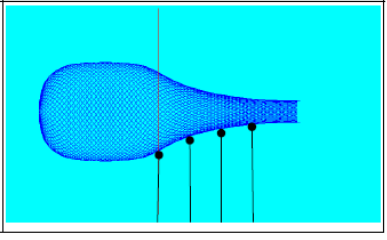

Fig. 5: plot of shapes for the cod-ends (design T0X100, T0X50, T90X100, T90X50 from top) for different catch weights (100 kg, 500 kg, 1000 kg from left). 1: marks edge of catch. 2: marks position 50 cm from catch edge. 3: marks position 100 cm from catch edge. 4: marks position 150 cm from catch edge.

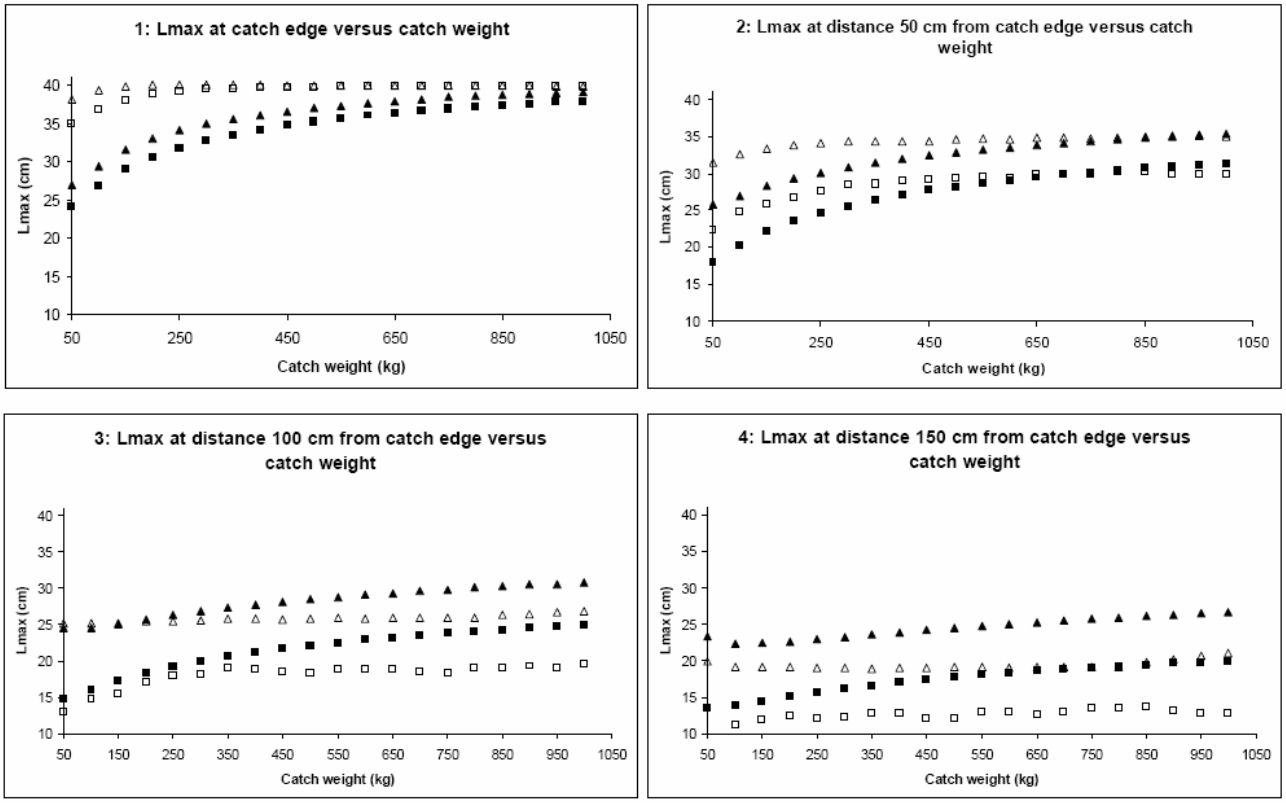

Fig. 6: *Lmax* for designs T0X100, T0X50, T90X100 and T90X50. 1: at catch edge. 2: 50 cm from catch edge. 3: 100 cm from catch edge. 4: 150 cm from catch edge. ■: design T0X100. □: design T0x50. ▲: design T90X100. Δ: design T90X50.

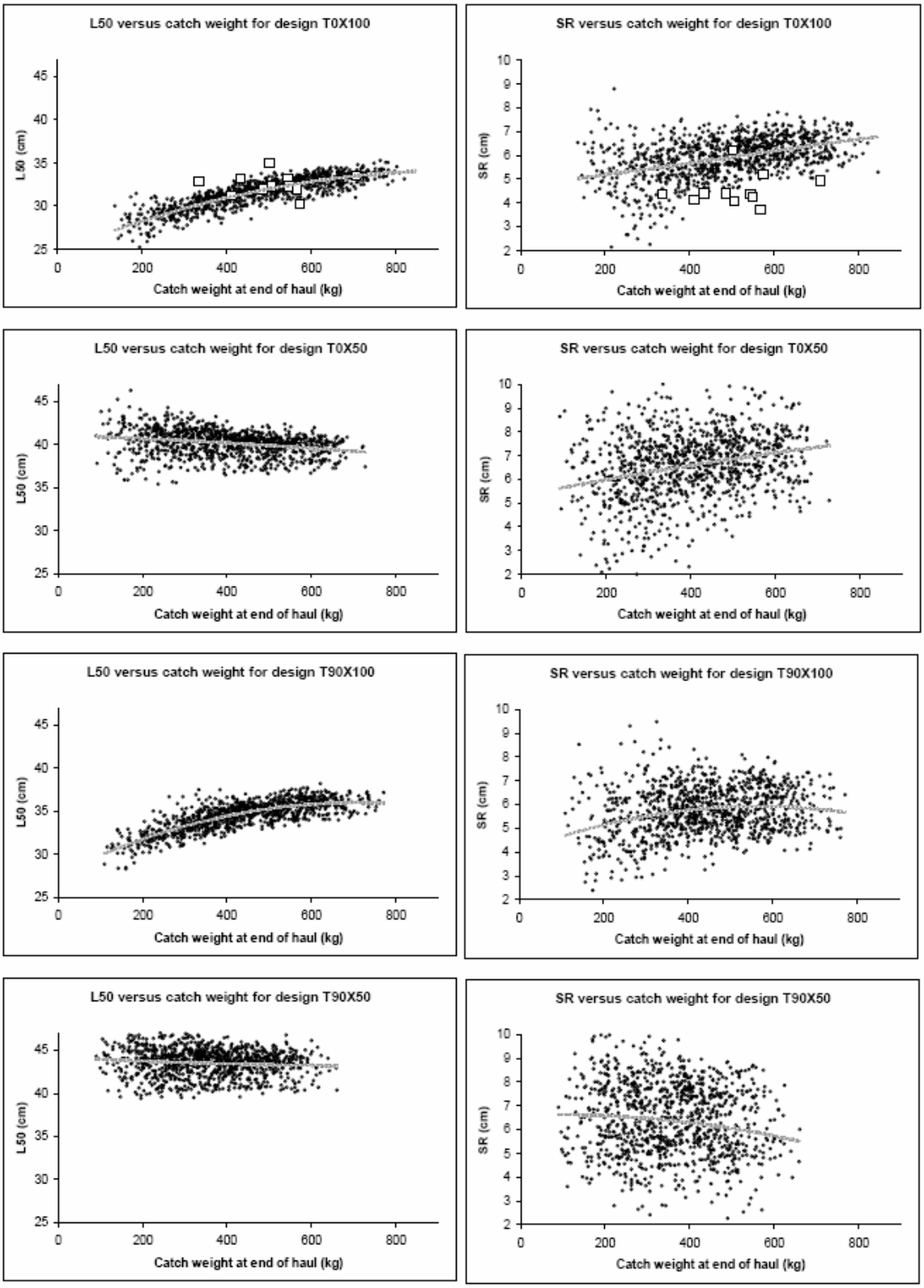

Fig. 7: L50 (left) and SR (right) versus catch weight at end of fishing for 1000 simulated hauls for each cod-end design T0X100, T0X50, T90X100 and T90X50 (from top). The curve is a second-order polynomial regression to the data. □ shown in the plots for design T0X100 (top row) represents single-haul results from Kynoch et al. (2003) but compensated (L50 + 2.1 cm, SR + 0.3 cm) for thicker twine based on model 4 in Herrmann and O'Neill (2006).

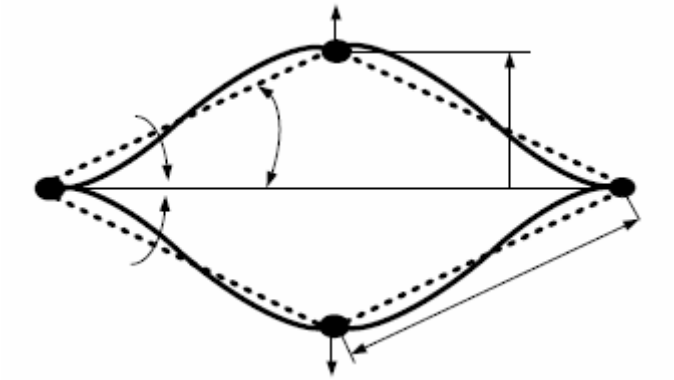

Fig. 8: Opening of diamond-mesh described by: i) bending beam bars as Sala et al. (2004) and O'Neill (1997) (full curves); ii) straight bars as FEMNET (broken lines). *Q*'s are a force couple to open the mesh which then counteracts with moments *C* to try to keep the mesh closed ($\Theta = 0$, $y = 0$). *m* is the full mesh size.

Table 1: Cod-end designs.

Cod-end design	Meshes in the circumference	Mesh orientation
T0X100	100	Normal
T0X50	50	Normal
T90X100	100	Turned 90°
T90X50	50	Turned 90°

Table 2: Factors in statistical model. I_1: reduction of meshes in the circumference. I_2: change in mesh orientation. I_3: both reduction of meshes in the circumference and change in mesh orientation.

Cod-end design	I_1	I_2	I_3
T0X100	0	0	0
T0X50	1	0	0
T90X100	0	1	0
T90X50	0	0	1

Table 3: Maximum escapement length (Lmax) versus catch weight at different distances from the catch edge. Lmax1: at catch edge. Lmax2: 50 cm from catch edge. Lmax3: 100 cm from catch edge. Lmax4: 150 cm from catch edge.

Catch Weight	Lmax1 (cm)				Lmax2 (cm)				Lmax3 (cm)				Lmax4 (cm)			
(kg)	T0X100	T0X50	T90X100	T90X50	T0X100	T0X50	T90X100	T90X50	T0X100	T0X50	T90X100	T90X50	T0X100	T0X50	T90X100	T90X50
50	24.1	34.9	26.9	38.1	18.0	22.3	25.8	31.5	14.7	13.0	24.5	25.2	13.4	9.9	23.3	19.9
100	26.8	36.8	29.4	39.3	20.3	24.8	26.9	32.6	16.0	14.7	24.5	25.2	13.8	11.3	22.3	19.2
150	29.0	38.0	31.5	39.8	22.2	26.0	28.3	33.3	17.3	15.5	25.1	25.2	14.5	11.9	22.4	19.1
200	30.5	38.8	33.0	40.0	23.6	26.8	29.3	33.8	18.3	17.1	25.7	25.4	15.1	12.4	22.6	19.2
250	31.8	39.2	34.1	40.0	24.7	27.7	30.1	34.1	19.2	18.0	26.3	25.5	15.7	12.2	22.9	19.0
300	32.8	39.4	34.9	40.0	25.6	28.4	30.8	34.3	20.0	18.2	26.8	25.6	16.2	12.3	23.2	19.0
350	33.5	39.6	35.5	40.0	26.4	28.6	31.4	34.4	20.6	19.1	27.3	25.8	16.6	12.8	23.6	18.9
400	34.1	39.7	36.0	40.0	27.1	29.1	32.0	34.4	21.2	18.8	27.7	25.8	17.0	12.8	23.9	19.0
450	34.7	39.7	36.5	39.9	27.8	29.2	32.5	34.4	21.7	18.6	28.1	25.7	17.4	12.1	24.2	19.0
500	35.2	39.7	37.0	39.9	28.2	29.3	32.9	34.6	22.1	18.3	28.5	25.8	17.8	12.1	24.5	19.1
550	35.6	39.8	37.3	39.9	28.7	29.6	33.2	34.7	22.5	18.9	28.8	25.9	18.1	12.9	24.8	19.1
600	36.0	39.8	37.6	39.9	29.1	29.5	33.5	34.6	22.9	18.9	29.1	25.8	18.3	13.0	25.0	19.0
650	36.3	39.8	37.9	39.9	29.5	29.9	33.8	34.8	23.2	18.8	29.3	25.9	18.6	12.5	25.3	19.1
700	36.6	39.8	38.1	39.9	29.8	29.8	34.1	34.9	23.5	18.6	29.6	26.0	18.8	13.0	25.5	19.2
750	36.9	39.9	38.4	39.9	30.1	29.9	34.3	34.7	23.8	18.3	29.8	25.9	19.0	13.5	25.7	19.1
800	37.1	39.9	38.6	39.9	30.4	30.2	34.6	34.8	24.0	19.1	30.1	25.9	19.2	13.6	25.9	19.2
850	37.3	39.9	38.7	39.9	30.7	30.3	34.8	35.0	24.3	19.1	30.3	26.3	19.4	13.7	26.1	19.8
900	37.5	39.9	38.8	39.9	30.9	30.0	35.0	35.1	24.5	19.3	30.5	26.5	19.6	13.2	26.3	20.2
950	37.7	39.9	39.0	39.8	31.1	30.0	35.2	35.1	24.7	19.1	30.6	26.7	19.8	12.8	26.5	20.7
1000	37.9	39.9	39.1	39.8	31.3	29.8	35.3	35.0	24.9	19.6	30.8	26.9	19.9	12.8	26.7	21.1

Table 4: Results of the simulations and comparison with empirical results. Galbraith A: predictions using model A in Galbraith et al. (1994). Galbraith B: predictions using model B in Galbraith et al. (1994). Compensated Kynoch: experimental results in Kynoch et al. (2003) compensated for their use of thicker twine (L50 + 2.1 cm, SR +0.3 cm) using model 4 in Herrmann and O'Neill (2006) (see text for details).

Cod-end design	Simulations		Galbraith A		Galbraith B		Compensated Kynoch	
	L50 (cm)	SR (cm)	L50 (cm)	SR (cm)	L50 (cm)	SR (cm)	L50 (cm)	SR (cm)
T0X100	31.6	5.9	30.9	5.6	30.2	6.9	32.5	4.5
T0X50	40.2	6.6	39.2	5.6	40.2	6.9	-	-
T90X100	34.5	5.7	-	-	-	-	-	-
T90X50	43.6	6.3	-	-	-	-	-	-

Table 5: Regression results for L50 and SR versus catch weight.

Catch weight	Design T0X100		Design T0X50		Design T90X100		Design T90X50	
(kg)	L50 (cm)	SR (cm)	L50 (cm)	SR (cm)	L50 (cm)	SR (cm)	L50 (cm)	SR (cm)
100	26.6	4.9	40.9	5.7	29.9	4.7	44.0	6.6
200	28.3	5.2	40.7	6.0	31.8	5.1	43.8	6.6
300	29.7	5.4	40.5	6.3	33.3	5.5	43.6	6.5
400	31.0	5.7	40.2	6.6	34.5	5.8	43.5	6.3
500	32.0	5.9	39.9	6.9	35.3	5.9	43.4	6.1
600	32.9	6.2	39.6	7.1	35.8	5.9	43.3	5.7
700	33.5	6.4	39.2	7.4	36.0	5.8	43.3	5.4
800	33.9	6.7	38.9	7.6	35.8	5.6	43.2	4.9

Table 6: Results for the statistical model.

		Estimate	sd	t-value	Dof	p-value
L50	$F_{0,1}$	31.66	0.049	649.51	7992	0.0000
	$F_{1,1}$	8.40	0.072	116.82	7992	0.0000
	$F_{2,1}$	2.84	0.070	40.74	7992	0.0000
	$F_{3,1}$	11.80	0.072	162.83	7992	0.0000
SR	$F_{0,2}$	5.86	0.038	152.55	7992	0.0000
	$F_{1,2}$	0.69	0.055	12.45	7992	0.0000
	$F_{2,2}$	-0.22	0.055	-3.93	7992	0.0001
	$F_{3,2}$	0.44	0.056	7.93	7992	0.0000

Table 7: Percentage effects of the single effects (i and ii) and the interaction between i and ii of the total effect. i: reduction of meshes in the circumference. ii: change of mesh orientation.

Factor	Factor effect of the total effect	
	Mean L50	Mean SR
i: reduction in number of meshes around	71%	155%
ii: 90 degrees change of mesh orientation	24%	-48%
interaction between i and ii	5%	-7%